RECENT DEVELOPMENT IN AMORPHOUS MAGNETISM

Supplement to Sci. Rep. RITU, A, June, 1978

RECENT DEVELOPMENT IN AMORPHOUS MAGNETISM

Noriaki.S. Kazama*, Neil Heiman

and Hiroshi Watanabe*

IBM Research Laboratory San Jose, California 95193

*The Research Institute for Iron, Steel and Other Metals, Tohoku University, Sendai, Japan

ABSTRACT

This report consists of five topics which have been recently developed by the authors in the amorphous magnetism, i.e., from the fundamental point of view, (i) magnetic properties of amorphous Fe alloys with Y, Lu, La and Zr are investigated, and the possible new magnetic structure will be presented. (ii) The concentration dependence of the Co moment and the concentration independence of the Co-Co exchange constant in amorphous alloys of Co with Y, La and Zr could be indicative of a localized virtual bound state of the Co moment. (iii) Magnetization process of amorphous RE_xCu_{1-x} alloys (RE=Tb, Dy, Ho and Gd) is also shown. From the application point of view, (i) amorphous Fe_xC_{1-x} ($0.75 \geq x \geq 0.50$) were prepared by sputter deposition. Room temperature values for $4\pi Ms$ ranged from 13000 gauss (x=0.75) to 6500 gauss (x=0.50). Thus the room temperature magnetization is much higher than that for amorphous alloys of Fe with other IV elements. We show that amorphous film of Fe-C can be prepared as low $Hc \approx 0.10$ Oe without the need for post deposition annealing by proper selection of the argon gas pressure. (ii) Effects of substrate bias and annealing on the properties of amorphous GdCo, GdFe and GdCoX (X=Mo, Au and Cu) films are investigated to control the magnitude of uniaxial magnetic anisotropy (Ku), which are useful for magnetic bubble device and magnetic-optic applications.

§1. MAGNETIC PROPERTIES OF AMORPHOUS Fe ALLOYS WITH Y, Lu,La AND Zr

INTRODUCTION

Most of the magnetic properties of amorphous heavy rare earth (RE)-transition metal (TM) alloys are complicated by the fact that (i) in amorphous structure every atomic site is not identical, this inequivalency results a wide distribution of exchange interaction in the TM owing to the dependence on distance, (ii) the consequence of this topological disorder is to bring into large crystal fields varing randomly in magnitude and direction, then it causes the uniaxial anisotropy which is significance for the RE atom, (iii) furthermore both RE and TM are contributing to the net magnetization and they couple antiparallel each other. As for the RE-RE interaction in amorphous RE-TM alloys it has been concluded to be ferromagnetic with nearly a half coupling strength of the crystalline RE metals on the basis of the experimental results of amorphous Gd-Cu[1], Gd-Ni and Ho-Ni[2] alloys. The addition of the RE atom into the amorphous TM, especially for amorphous Fe which has supposed to be complex spin structure with an average z-component per atom of about $0.8\mu_B$[3] (and $Tc \approx 200K$), is to straighten up a nearest neighbor TM antiparallel through the antiferromagnetic exchange interaction.[4] Finally concerning to the TM-TM interaction, it plays a significant role in amorphous RE-TM alloys. For example the Fe-Fe coupling constant is one of the strongest among amorphous RE-TM alloys and increases with increasing RE concentration, furthermore the magnetic moment of Fe depends strongly on the concentration of RE and its effective spin in the amorphous alloys than in the crystalline alloys.[5][6] Since there is no systematic experimental data concerning to this important TM-TM interaction isolated from other additional effects, we have undertaken the task of examining the interaction by preparing amorphous Fe alloys with Y, Lu, La and Zr.

EXPERIMENTAL PROCEDURE AND RESULTS

In order to isolate the Fe-Fe interaction and evaluate the effect of non-magnetic RE atoms on Fe, we have measured the magnetic properties of the Fe-based amorphous alloys with La, Y, Lu and Zr, which are gradually decreasing in the atomic size from 1.87 Å for La to 1.60 Å for Zr. These amorphous films were prepared by the coevaporation method of each element. Films were determined to be amorphous state by x-ray diffraction, however some of the higher Fe concentration films, i.e., $La_{0.19}Fe_{0.81}$ and $Zr_{0.12}Fe_{0.88}$ were found to be partially crystalline through the x-ray examination. The chemical composition of all films were determined by electron probe x-ray microanalyzer techniques for thin films. The accuracy of the results is expected to be better than 5 atomic % (at.%) relative. Magnetization measurements were carried out from 4.2K to 300K on a vibrating sample magnetometer in fields up to 20KOe and the Mössbauer effects were also examined.

RESULTS

A. Y-Fe

Amorphous films of $Y_{1-x}Fe_x$ were prepared with x=0.70, 0.75, 0.83. Whereas the crystalline Y-Fe alloys are normal ferromagnets, the M vs. H curves of the amorphous samples failed to saturate even in high fields as illustrated by Figure 1-1.

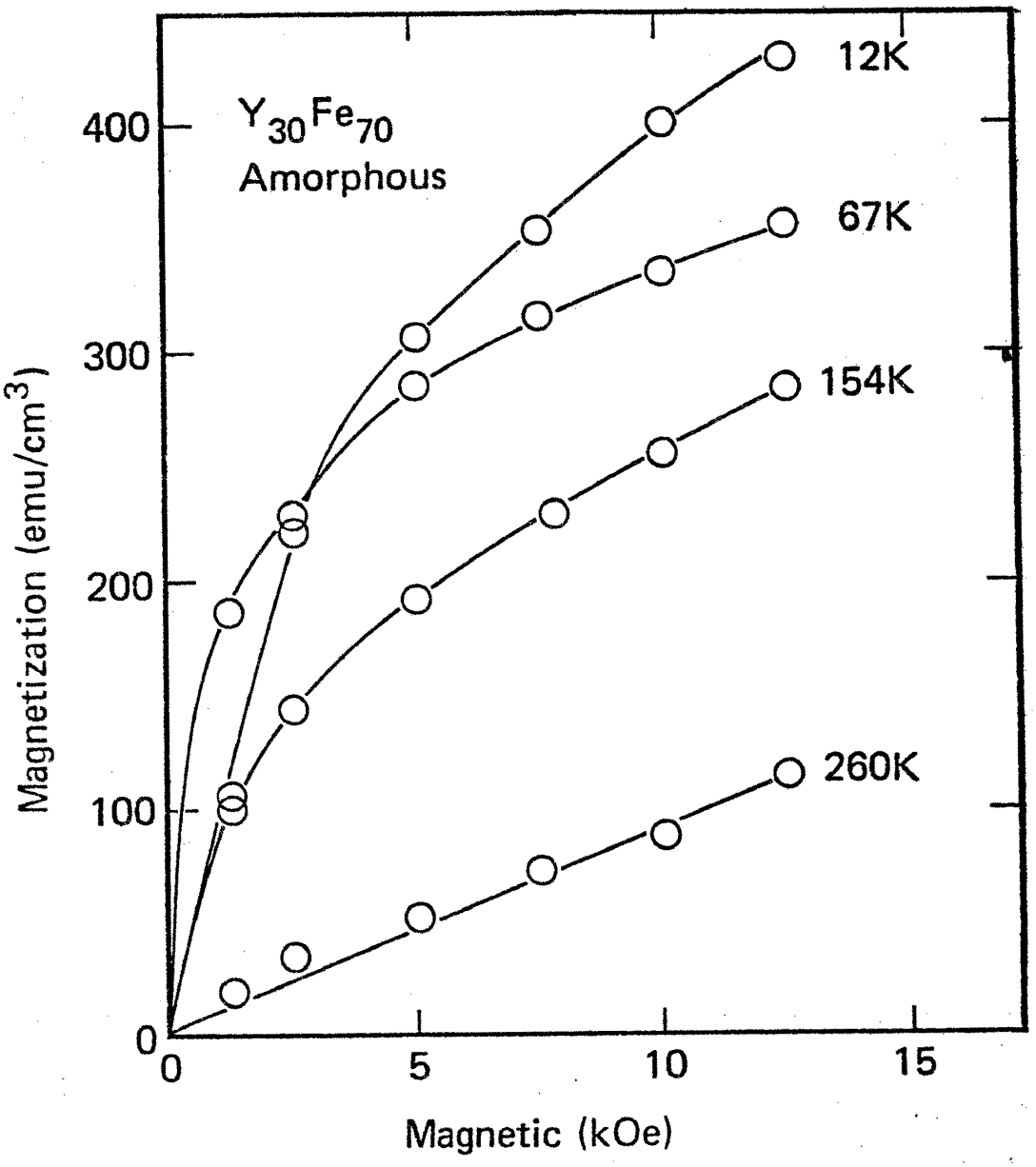

Fig. 1-1. Field dependence of the magnetization at several temperatures for a sample of amorphous $Y_{0.30}Fe_{0.70}$. Note the lack of saturation.

A plot of M vs. temperature (T) is shown in Figure 1-2 for a sample with x=0.70.

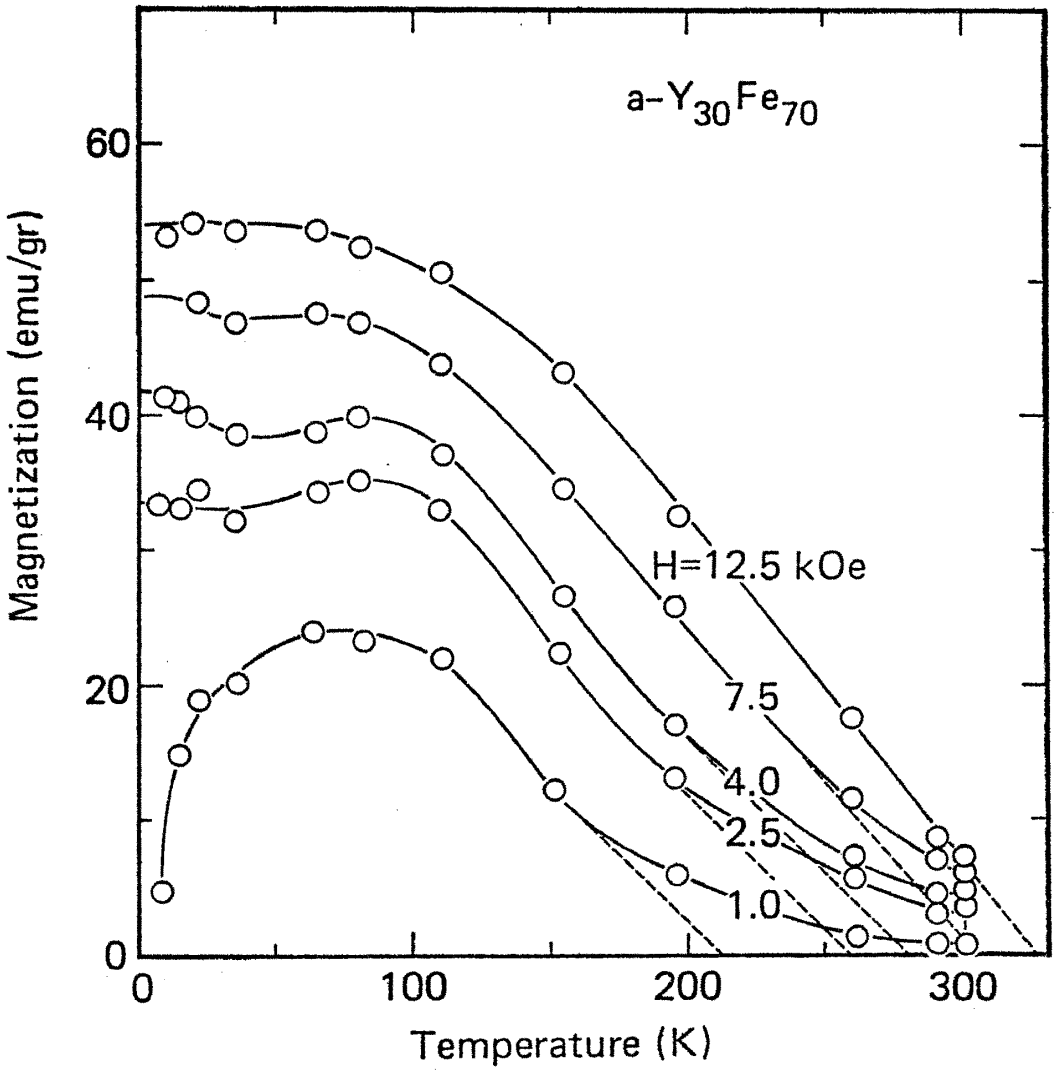

Fig. 1-2. Temperature dependence of the magnetization at several applied fields for the same sample shown in Figure 1-1. Note the strong field dependence. Although the samples are not ferromagnetic, one may attempt to define field dependent ordering temperature by linear extrapolation of M to M=0 (dashed lines).

The M vs. T behavior is clearly a strong function of applied field. In high applied fields M decreased gradually with T over the entire range from 4.2K to 300K and showed no sharp transition. As the applied field is lowered, M vs. T behavior is strange, first rising with increasing T and then decreasing. This is suggestive of spin glass behavior.

We can assign an average Z component for the moment of the atom from M at 4.2K and H=12.5kOe by assuming the alloy density to be linear combination of the elemental densities in proportion to the elemental concentrations, i.e., $\rho_{alloy}=x\rho_{Fe} + (1-x)\rho_{Y}$. Such a procedure yields $\mu_Z \simeq 0.9\mu_B$ with little dependence on concentration. If we extrapolate μ_Z to H=∞, we find only a slight increase to $\mu_Z \simeq 1.05\mu_B$.

Mössbauer spectra at 4.2K show a broad six line pattern. No attempt was made to deconvolute the spectrum into a distribution of magnetic hyperfine fields (H_{hf}). The spectrum could be fit quite well with an average $\bar{H}_{hf}$ and lines broadened in proportion to the Zeeman energies.

It is enlightening to plot $\bar{H}_{hf}$ and μ_{Fe} for the amorphous alloys on the same figure with data for crystalline Y-Fe alloys.

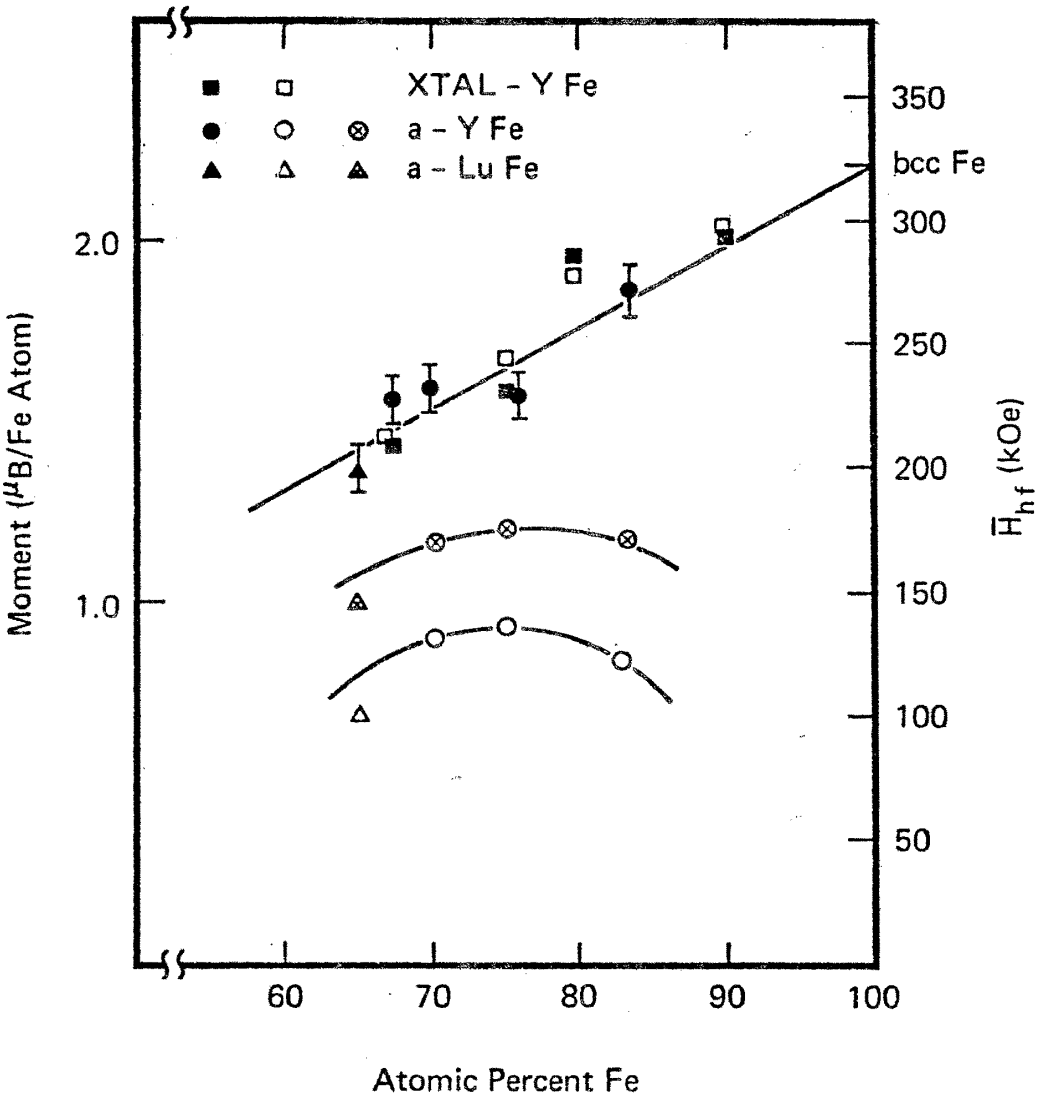

Fig. 1-3. Average hyperfine field ($\bar{H}_{hf}$) and moment per Fe atom obtained from magnetization measurements for both crystalline and amorphous YFe alloys. Note that for the amorphous alloys, the moments per Fe atom obtained from $\bar{H}_{hf}$ are comparable to those for crystalline YFe alloys (whether obtained by $\bar{H}_{hf}$ or magnetization measurements). However, the moments per Fe atom for the amorphous alloys obtained by magnetization measurements are much less. This suggests that the average Fe moments are the same in crystalline and amorphous alloys but are not aligned in the amorphous state (spin glass).

It is clearly seen that $\overline{H}_{hf}$ for the amorphous alloys is nearly identical to that of the crystalline alloys. This suggests strongly that the atomic moments are the same in the crystalline and amorphous alloys. On the other hand μ_{Fe} obtained from magnetization data show a fairly reduced value. The combined results suggest that in the amorphous alloys, the magnetic structure is one of the "spero-magnetic" structures. The most likely reason for this is large fluctuations in the value of the Fe-Fe exchange interactions.

The composition dependence of T_c can be seen in Figure 1-4. For composition we have included T_c for the crystalline alloys.

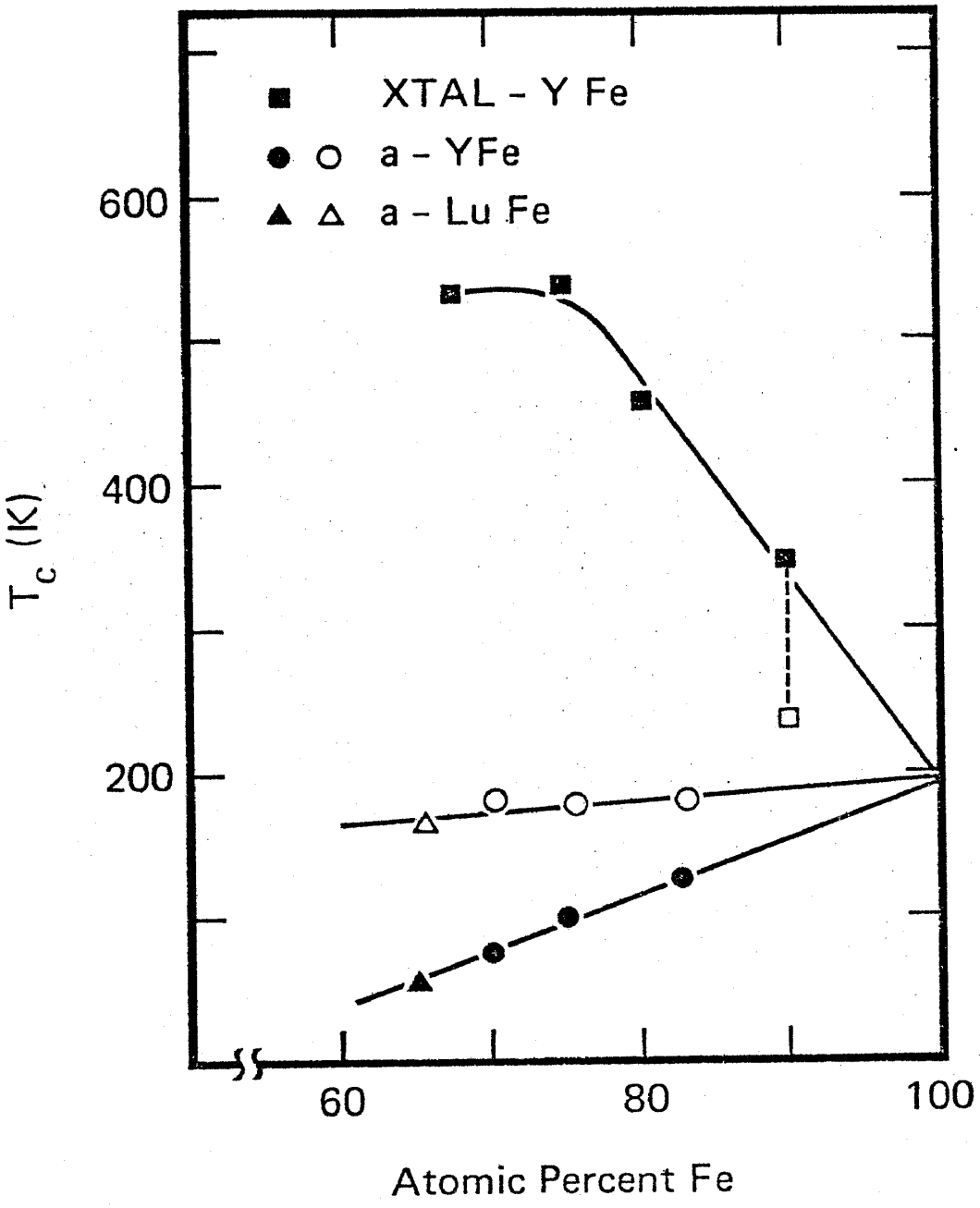

Fig. 1-4. Ordering temperature for amorphous and crystalline YFe alloys. The solid squares are the result for crystalline alloys. The solid circles are the result for the amorphous alloys obtained from Mössbauer effect data. The open circles are the result obtained from magnetization data extrapolated to H=0. The triangles, the result for $Lu_{0.35}Fe_{0.65}$, are included for comparison.

Values for T_c in the crystalline case are essentially the same whether obtained from magnetization measurements or from Mössbauer effect determinations. However this is not for the amorphous Y-Fe alloys. If we attempt to define a T_c as the temperature at which a linear extrapolation of M intersects M=0 (as indicated by the dashed lines in Figure 1-2), we arrive at a T_c which is strongly field dependent. These facts may explain the wide variation of reported T_c values for these alloys.

An interesting observation is that the extrapolation of T_c to pure Fe yields $T_c \approx 200K$ for both the crystalline and amorphous systems. If we use the mean field formula:

$$J_{Fe} = \frac{3kT_c}{2zxS(S+1)} ,$$

where k is Boltzman's constant, z is the coordination number (assumed to be 12) and x is the Fe concentraion . We can assign J_{Fe} values. It is interesting to consider two cases: (1) T_c and S^{Fe} determined from $\bar{H}_{hf}$ and (2) T_c and S determined from magnetization measurements. Using the values determined from Mössbauer effect measurements, one finds $J_{Fe} \simeq 1.7 \times 10^{-15}$ ergs for all values of x, i.e., is independent of Fe concentration. This result is similar to the result reported by us for amorphous Y-Co alloys. Such a result is evidence that long range interactions and structure effects are absent in the amorphous materials and J depends only on pairwise nearest neighbor exchange. It is also interesting to compare this result to the situation for crystalline YFe compounds where J_{Fe} rises steeply with the addition of Y. The difference is striking evident in Figure 1-5.

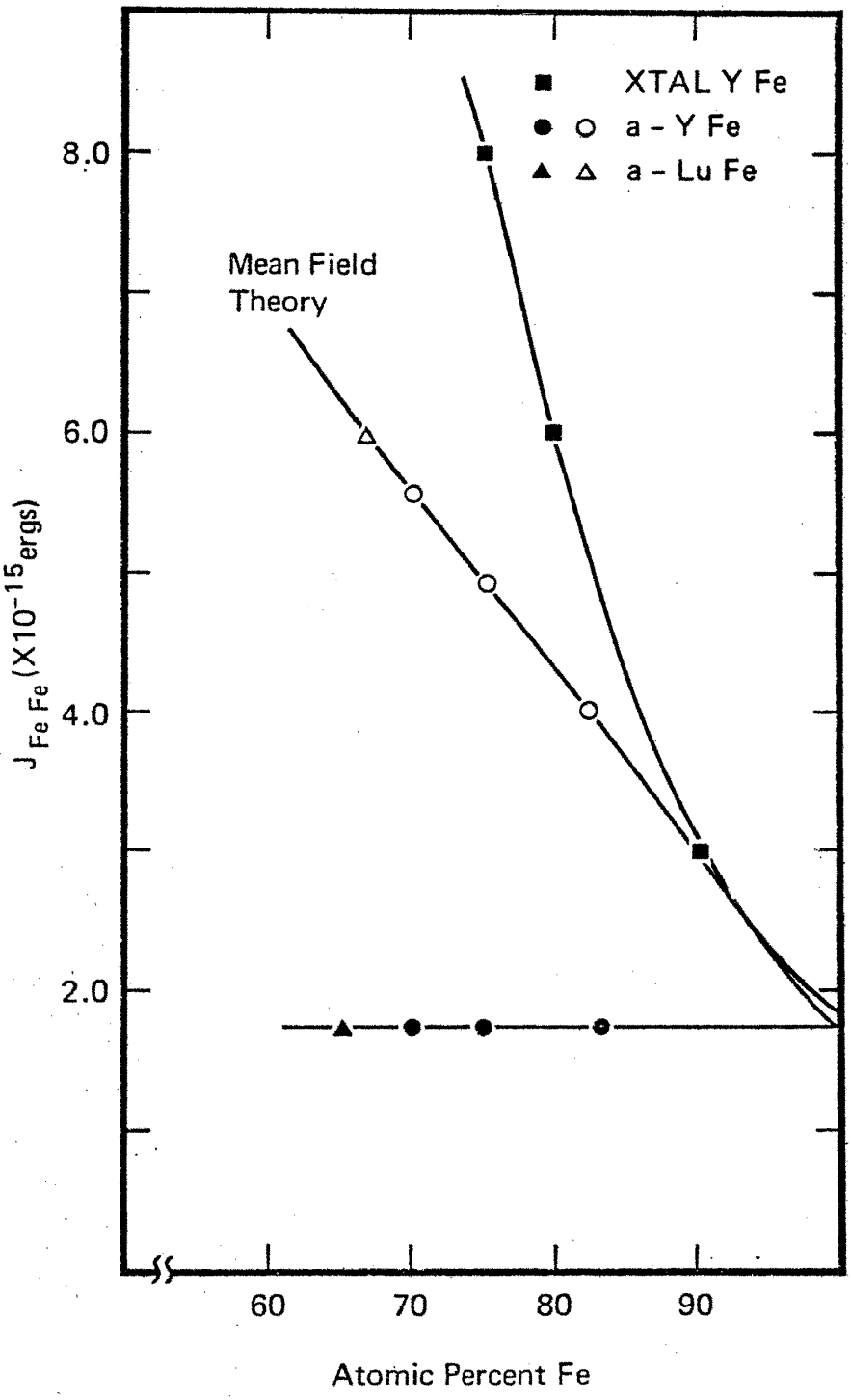

Fig. 1-5. Exchange constants for crystalline and amorphous YFe alloys as calculated in the text. Solid squares are the result for crystalline alloys. The solid circles are the result for the amorphous alloys obtained from Mössbauer effect data. Note that J_{FeFe} is a constant. The result implies only nearest neighbor interactions are important. The open circles are from magnetization data and presumably not valid but are included to illustrate that they agree with mean field predictions of Heiman et al. Results for LuFe (triangles) are included for

comparison.

B. Lu-Fe

We prepared only one composition-$Lu_{0.38}Fe_{0.62}$. The results for the magnetic properties of amorphous $Lu_{0.38}Fe_{0.62}$ were similar to and consistent with those for amorphous Y-Fe. The results are included in Figures 1-3, 4, 5.

C. La-Fe

Amorphous films of $La_{1-x}Fe_x$ were prepared with x=0.69 and 0.76. Films with higher Fe content were found to show the presence of crystalline Fe. Unlike the results for the amorphous Y-Fe alloys, the magnetization of the amorphous alloys were easily saturated in low applied fields and T_c does not depend strongly on applied fields. We find that M(T) does not obey a simple molecular field model law. This suggests that exchange fluctuations are fairly large.

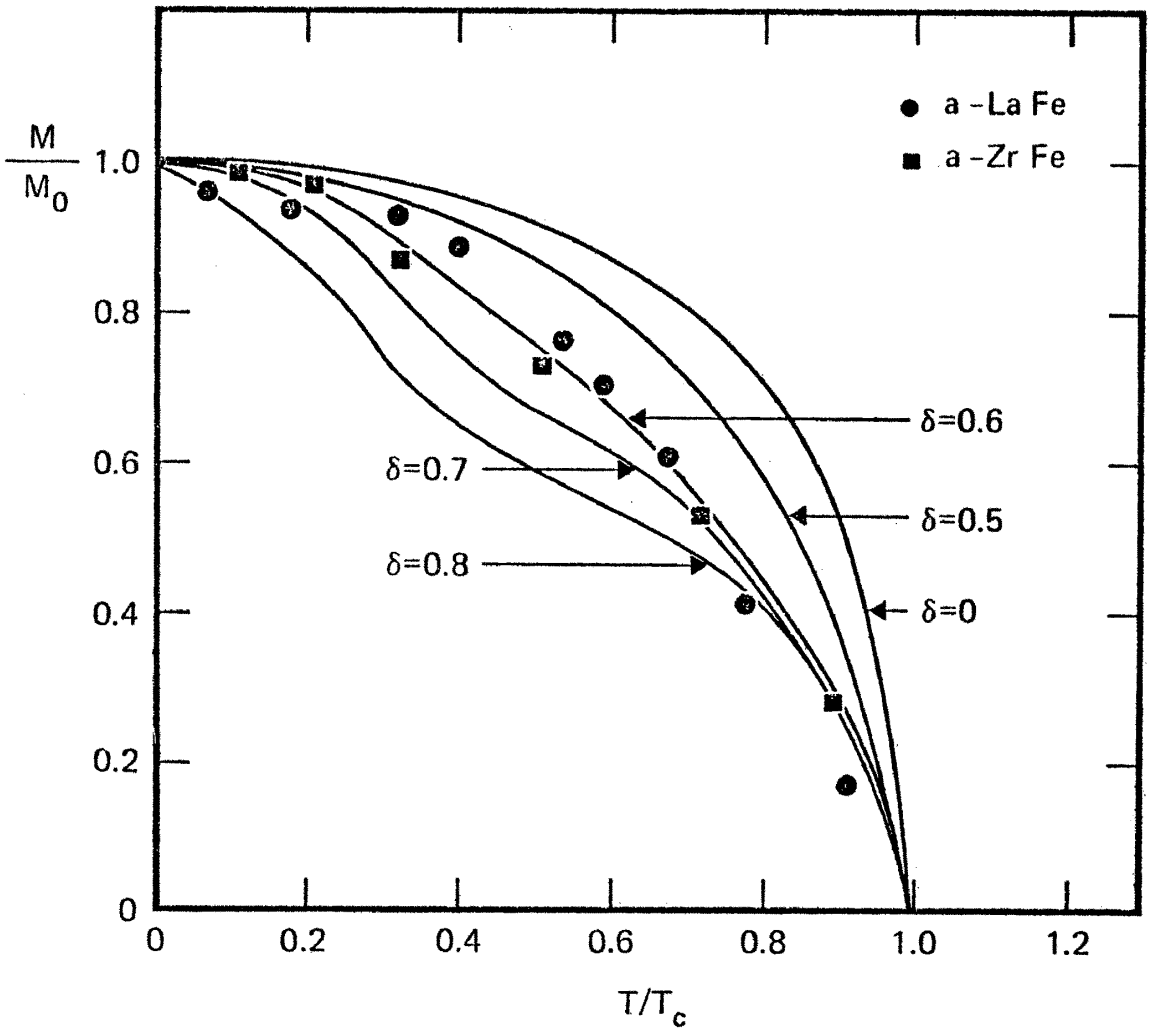

Fig. 1-6. Normalized magnetization vs. temperature behavior according to Handrich model for various ratios of exchange fluctuations to exchange i.e., $\delta=\Delta J/J$. The data for amorphous LaFe and ZrFe yields $\delta\approx 0.6$.

D. Zr-Fe

Amorphous films of $Zr_{1-x}Fe_x$ were prepared with x=0.65, 0.76 and 0.80. The magnetization of all samples saturated easily in low applied fields. The agreement between μ_{Fe} from magnetization data and that from Mössbauer effect is within statistical error. The data are summarized in Fig. 1-6,7.

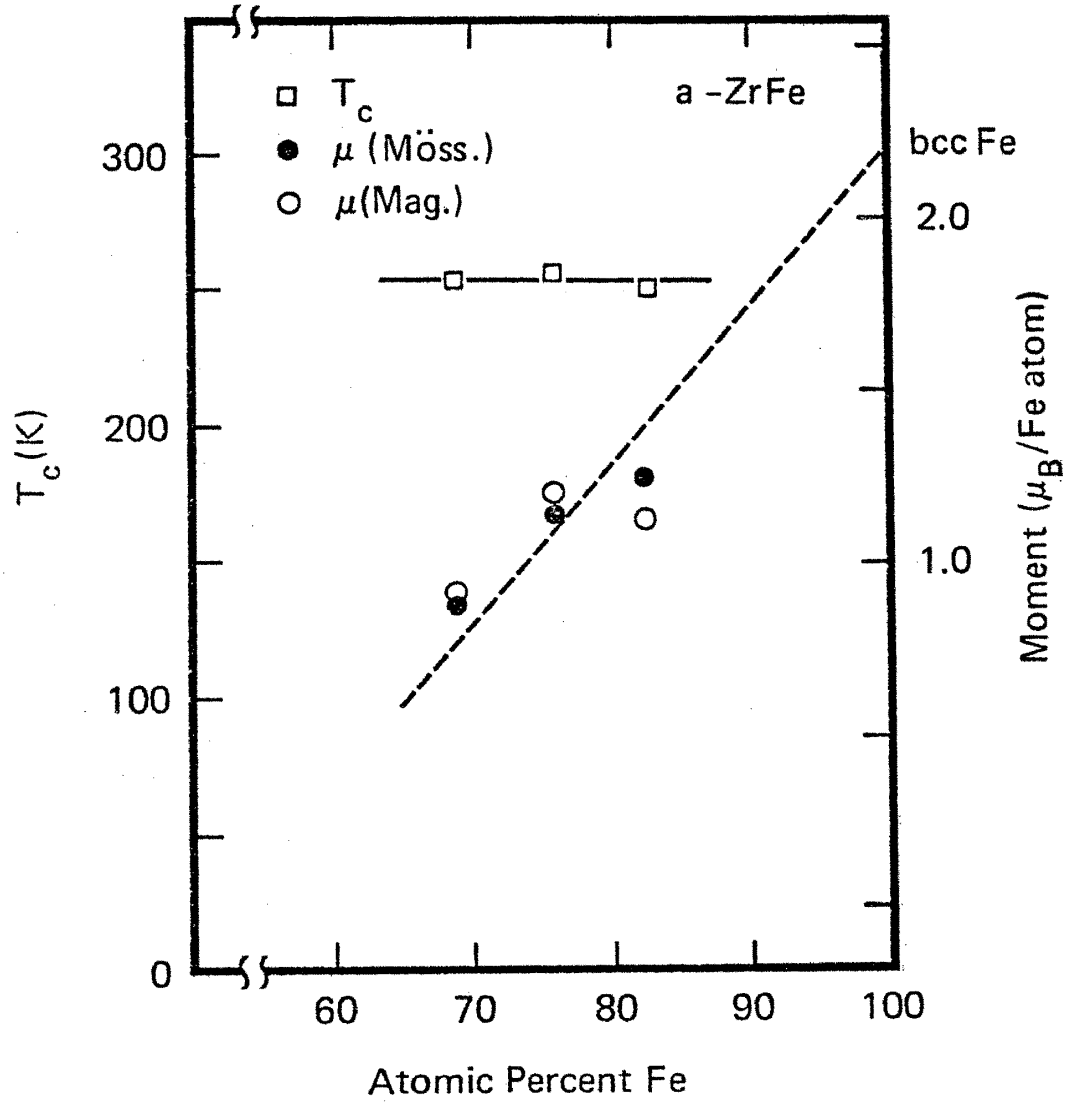

Fig. 1-7. Magnetic moment per Fe atom and T_c for amorphous ZrFe alloys. Note approximate agreement between Mössbauer effect result and magnetization result. T_c was also the same by both methods.

§2. THE CONCENTRATION DEPENDENCE OF THE Co MOMENT IN AMORPHOUS ALLOYS OF Co WITH Y,La AND Zr

The concentration dependence of the Co moment has been measured in amorphous $Y_{1-x}Co_x$, $La_{1-x}Co_x$ and $Zr_{1-x}Co_x$ alloys ($0.33 \lesssim x \leq 0.88$). For the amorphous alloys systems, they are "well defined" ferromagnets but the concentration of Y, La, or Zr at which the Co moment disappear is much higher than for the crystalline systems as shown in Fig. 2-1. Furthermore the critical concentration is the same for Y and La[$(1-x) \gtrsim 0.5$] but lower for Zr[$(1-x) \approx 0.4$].

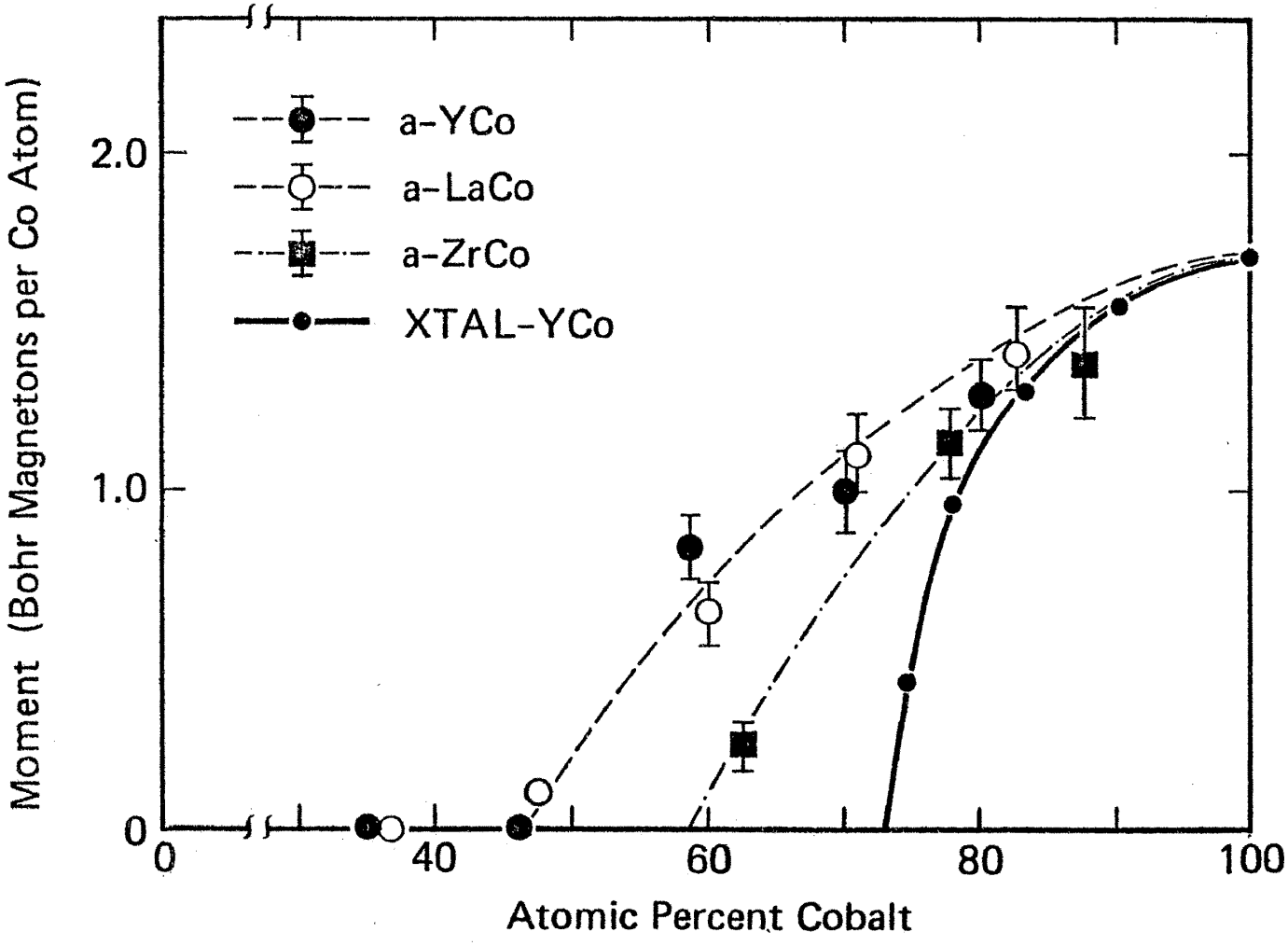

Fig. 2-1 The figure shows the concentration dependence of the Co moment for the amorphous Y-Co, La-Co and Zr-Co alloys. The heavy solid line shows the concentration dependence of the Co moment for the crystalline Y-Co alloys taken from the reference [7]. (the data for crystalline La-Co alloys is nearly identical). The broken lines are intended merely to indicate the trend of the data.

Since Y and La are expected to have the same valence (nominally 3^+) but have different atomic radii (R_{La}=1.87 Å and

R_Y=1.80 Å R_{Gd}) and Zr, though smaller than Y, (R_{Zr}=1.60 Å) is expected to be of a higher valence state (nominally 4^+), the result that Y and La yield similar data indicates that the size of the non-magnetic atom does not play a significant role in the magnetic properties. This is in contrast to the results for the amorphous YFe and LaFe alloys.

The lower critical concentration for the Zr alloys suggests a charge transfer mechanism for the reduction of the Co moment upon alloying. However the reduced charge transfer is by no means the only interpretation of the data available. In the discussion of a virtual bound state model,[8] it has been shown that the concentration dependence of the Co moment is expected to vary as $(x-x_o)^{1/2}$, where x_o is some critical concentration.

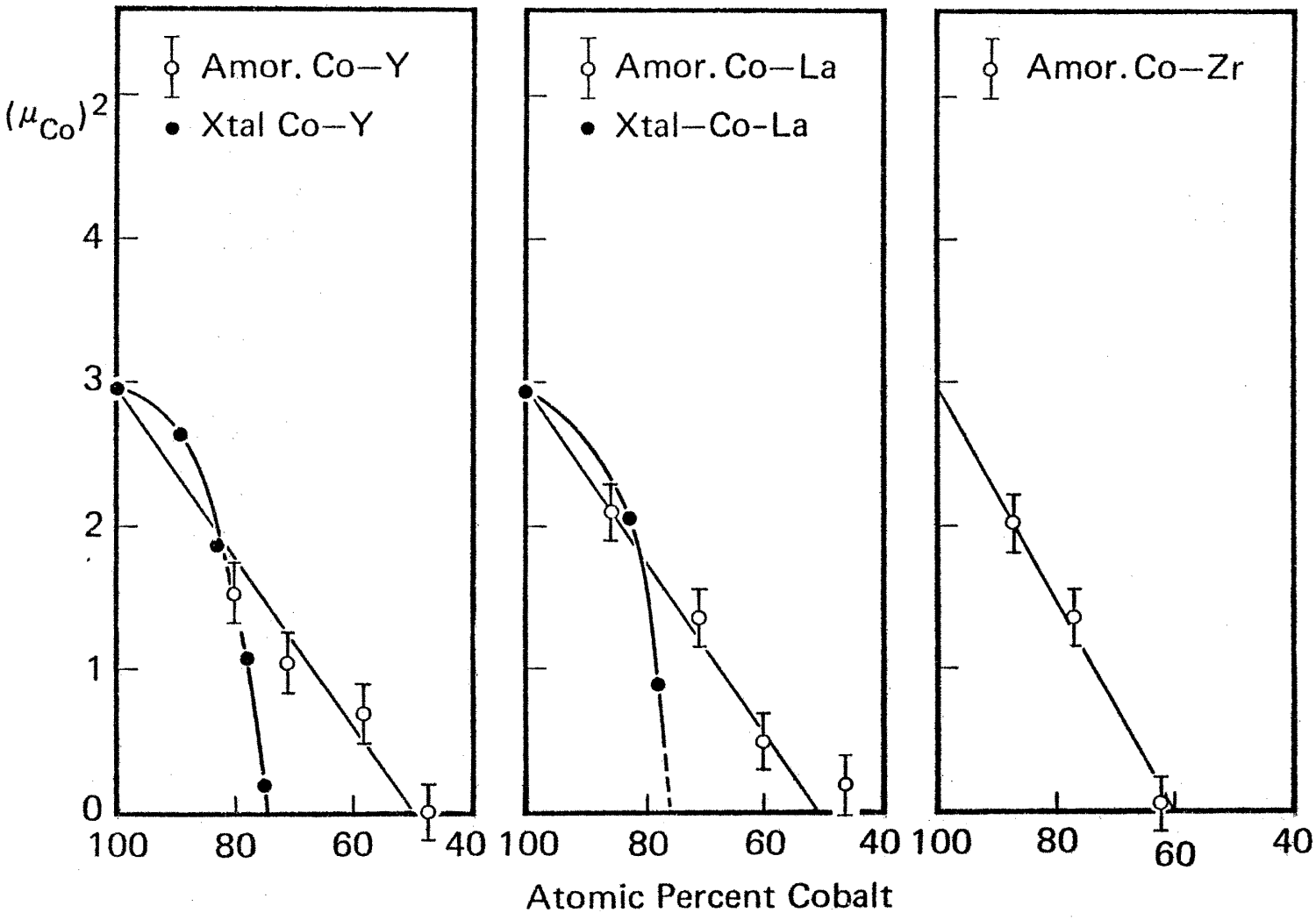

Fig. 2-2 In this figure the square of the Co moment is plotted against Co concentration for both the crystalline and amorphous alloys.

It is interesting to note that the amorphous data can be described by a straight line whereas the crystalline data

cannot.

The fact that the resistivity of these alloys is very large[9] ($\rho \approx 200\mu\Omega$-cm at room temperature) indicates an electron mean free path of the order of the atomic spacing. Thus a more localized picture would seem appropriate for the amorphous alloys.

One argument which seems to support for a localized picture comes from the behavior of the Co-Co exchange constant (J_{Co}). Using the formula $J_{Co}=3kTc / 2Z \cdot S(S+1)$, where $Z=12x$ is the average number of Co nearest neighbors. The result is shown in Fig. 2-3.

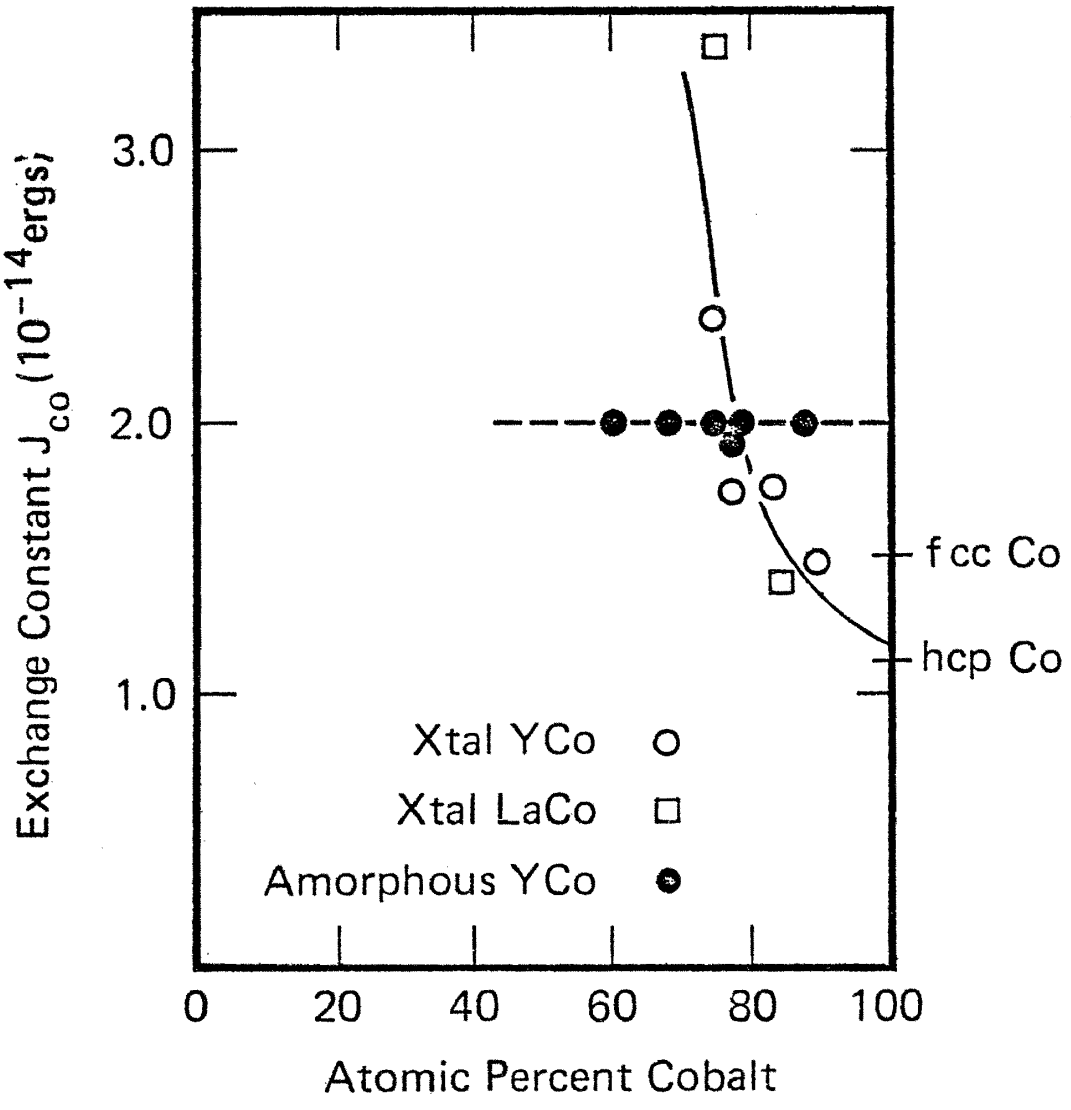

Fig. 2-3. The figure shows the concentration dependence of the Co-Co exchange constant (J_{Co}).
Although J_{Co} increases upon alloying the in the crystalline case, it is independent of the concentration for the amorphous alloys. ($J_{Co} \approx 2.0 \times 10^{-14}$ ergs). It is also the same value as the results calculated from amorphous Co-metalloid alloys[10] This is consistent with the idea that long range interactions

or structure effects are absent in the amorphous materials, and that J_{Co} depends only on pair-wise nearest neighbor exchange. This result is thus consistent with a more localized moment behavior in the amorphous alloys than the crystalline ones.

§3. MAGNETIZATION OF AMORPHOUS RE_x-Cu_{1-x} ALLOYS

(RE=Tb, Dy, Ho, Gd)

Recent theoretical work has dealt with the effects of random crystal fields on the magnetic properties of amorphous magnetic materials. Most of the work has been directed toward explaining the somewhat coercive force type magnetization in amorphous $TbFe_2$. There are complication which arise in this materials as well as other amorphous rare earth (RE)-transition metal (TM) alloys in that strong exchange fluctuation of the Fe subnetwork produce effects which often mask any random crystal fields effects. To eliminate these difficulties, we have prepared samples of $RE_{1-x}Cu_{1-x}$ alloys where RE=Gd, Tb, Dy, Ho and $0.30 \leq x \leq 0.60$. Cu was selected because it is a non magnetic 3d transition metal so that the only magnetic atom are RE. The RE and composition ranges were selected to provide a variation in the parameter D/J, which is the ratio of the single ion uniaxial anisotropy to the exchange constant. J may be expected to show only a small variation with RE and x, but D will vary greatly due to the large variation in the Steven's factor for the RE. (The Steven's factor is the effective coupling of the RE to the crystal field).

Gd is an S state atom, and thus local anisotropy effects should be absent in these alloys. Tb and Dy both have very large Steven's factors, so one expects local anisotropy effects to be most apparent in alloys containing these elements. Ho is an intermediate case.

GENERAL

The values for each RE species with various x are shown in table 1 in units of Bohr magneton (μ_B), where M_S is the magnetization one calculate for aligned spins with the full value of gJ.

Table I

RE	Gd		Tb		Dy		Ho	
Stevens Factor	0		66		63		24	
	M/MS	H_c (kOe)	M/MS	H_c (kOe)	M/MS	H_c (kOe)	M/MS	H_c (kOe)
x = 0.6	1.00	–	0.60	21.0	0.56	10.5	0.63	(4.3)
x = 0.5	0.93	–	0.45	14.0	0.60	7.0	0.65	(2.0)
x = 0.4	(0.78)	–	0.41	8.8	0.48	5.2	0.84	(2.6)
x = 0.3	0.98	–	0.41	(3.5)	0.53	(2.6)	0.72	(1.3)
Average	0.92	–	0.47	11.8	0.55	6.3	0.71	(2.5)

Two features are readily apparent in table 1. First the sample containing Gd (a S state atom) develops its full moment while the Tb, Dy and Ho samples have greatly reduced magnetization. Furthermore the reduction from full moment among these samples is in order of the Steven's factor of the RE, with Tb having the largest Steven's factor and Ho the lowest. Secondly the these non-S state samples develop large coercive forces and the magnitude of the coercive force among the samples is also in the order of the Steven's factors. This seems to be indisputable evidence that both of these effects are due to anisotropy.

$$Gd_xCu_{1-x}$$

As noted, Gd is a S state atom so no anisotropy effects are expected and none were observed. With the exception of x=0.40 (which for some reason has an anomalously low M), one obtains a magnetization consistent with the full gJ moment. All samples behave as expected for normal ferromagnetic coupling (except for x=0.30). This is in contrast to the crystalline GdCu alloys, all of which have antiferromagnetic coupling. The Curie temperature were obtained from the M vs. T behavior and are plotted in Fig.3-1, along with data reported for other amorphous Gd alloys.

The general disappearance of good ferromagnetic behavior in this range is a strongly indication of a percolation limit. In a Heisenberg statistic nearest neighbor model,

$$\frac{kT_c}{J} = \frac{2}{\ln\left(\frac{xz}{xz-4}\right)},$$

where z is the coordination number. The percolation limit occurs for $x_o=z/4$. This is the concentration at which ferromagnetism disappears because of the formation of clusters containing Gd which no longer have continuous nearest neighbor coupling to the bulk. If z is taken to be 12 as is the usual choice for these amorphous alloy one finds the percolation limit is $x_o \approx 0.33$. The solid line in Fig. 3-1 is a fit to this percolation theory. The fit is convincing evidence of a statistical nearest neighbor model. The result of the magnetic specific heat of amorphous $GdAl_2$[23] suggests that the dominant excitations at low temperature are short-wavelength ferromagnetic spin-waves. They are excited in small regions of size approximately 35 Å where the magnetic order has a significant ferromagnetic component. The direction of the net moment varies from one cluster to the next. This situation seems to be occured for the sample x=0.30 in which we were unable to find clear T_c. Localized nearest neighbor model has been proposed for most of the amorphous RE-TM alloys. In the case TM= Fe or Co, a simple percolation model is not applicable because the TM moment disappears. Here, of course, the Gd moment is uneffected by concentration, and percolation theory works well. This result in turn supports the localized picture for the other amorphous alloy systems.

One final point is that the $T_c \approx 200K$ for amorphous Gd metal obtained from this model is consistent with the mean field model prediction of others.

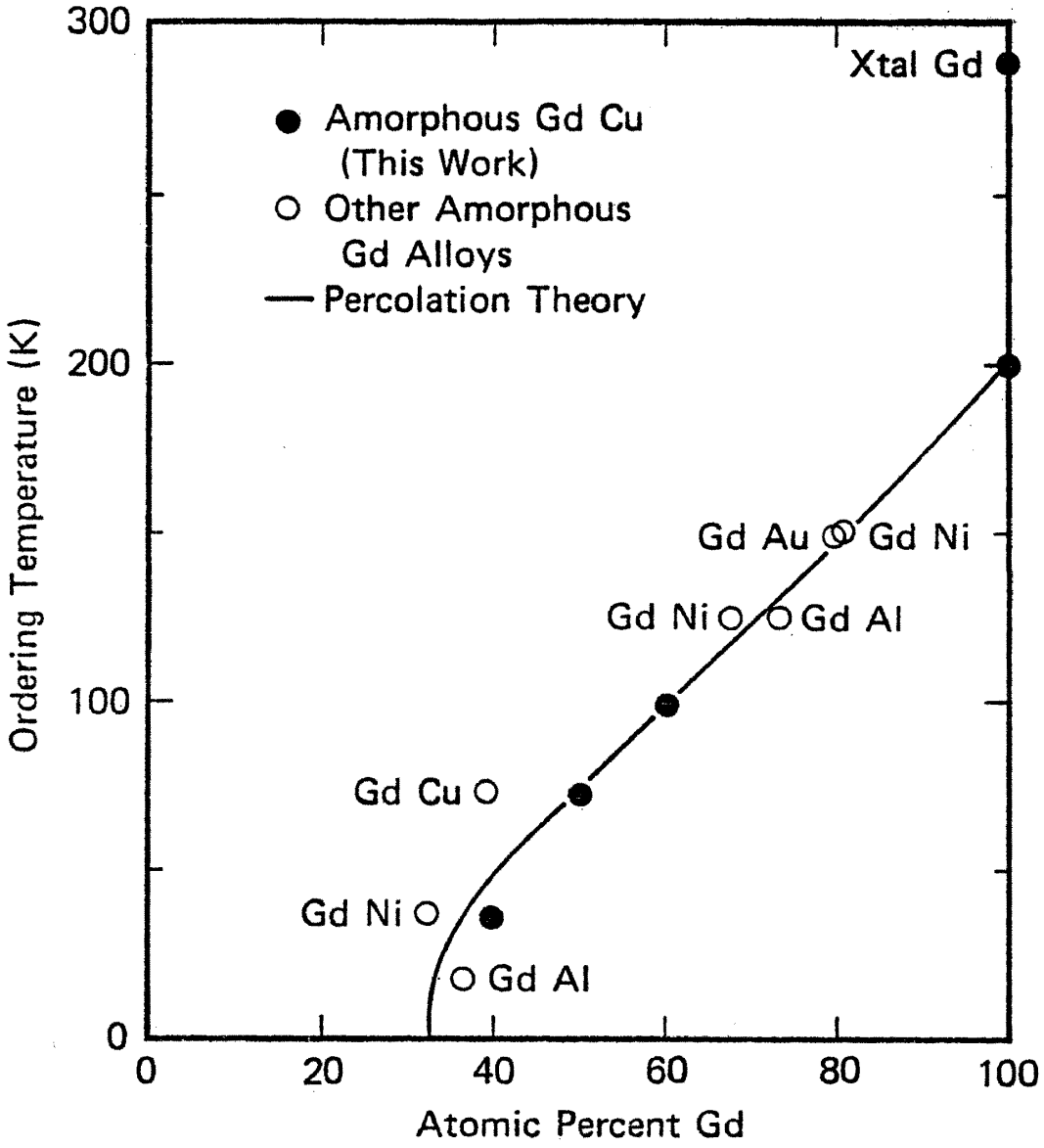

Fig. 3-1. T_c vs concentration for amorphous. Gd_xM_{1-x} alloys, where M is a nonmagnetic metal. Addition points are obtained from Ref. 11, 12, 13 and 14. The solid line is a statistical nearest neighbor theory with a percolation limit of x=0.33.

§4. MAGNETIC PROPERTIES OF AMORPHOUS Fe-C ALLOYS

It is well known that rapidly quenched bulk amorphous transition metal-metalloid alloys can be made with high permeability, low coercivity, and in some cases low magnetostriction; however little is known of the magnetic properties of these alloys when prepared as thin films. In addition to the technological advantages, it is expected that thin film deposition techniques should be more effective in producing the amorphous state. Thus it should be possible to extend the range of materials which can be produced. This could prove important in obtaining more fundamental understanding of these glassy systems. In particular, most of the reported bulk amorphous metal-metalloid systems contain two or more metalloids and generally do not deviate greatly from 80 at.% transition metal-20 at.% metalloid composition ratio. Thin film techniques should result in the production of several binary combinations with wide composition ranges. Shimada and Kojima[15] and Marchal et al.[16),17)] have already explored amorphous thin films of Fe_xSi_{1-x}, while Suran et al.[18),19),20)] have investigated amorphous Fe_xGe_{1-x} films. There are a number of differences between the Fe_xC_{1-x} and previous Fe_xSi_{1-x} or Fe_xGe_{1-x} films. One of the most significant differences is that unlike the earlier materials the Fe_xC_{1-x} films can be prepared with $Hc<100mOe$ and thus have potential applications in the area of soft magnetic films.

A. CONCENTRATION DEPENDENCE OF THE MOMENT AND CURIE TEMPERATURE

The most striking result was that both the magnetic properties and the compositions of the films were a strong function of Ar gas pressure (P_{Ar}). This presented a complication in terms of charactering these films since initially it was not clear which features were due to deposition conditions and which were due to composition changes. The effect of P_{Ar} on composition is shown in Fig. 4-1 (note that the abscissa is on a log scale). At very low pressure ($P_{Ar} \to 0$), the film composition is near target composition. As P_{Ar} is increased, the films become Fe deficient (or C rich); and the effect is quite large. Thus with only two targets we can span the range $0.75 \geq x \geq 0.50$. It should also be noted that, because the films were deposited with all deposition parameters fixed except P_{Ar}, the rates increase as P_{Ar} increases. Thus either high pressure or high rate may be responsible for the Fe depletion (or C enrichment). We have also deposited other amorphous metal-metalloid combinations such as Fe-Cr-P-C and Fe-Si-B (see Figs. 4-5, 6. These are the subject of another paper[21)]) and find that there is very little P_{Ar} dependence to the composition. Thus this effect seems confined to C based alloys.

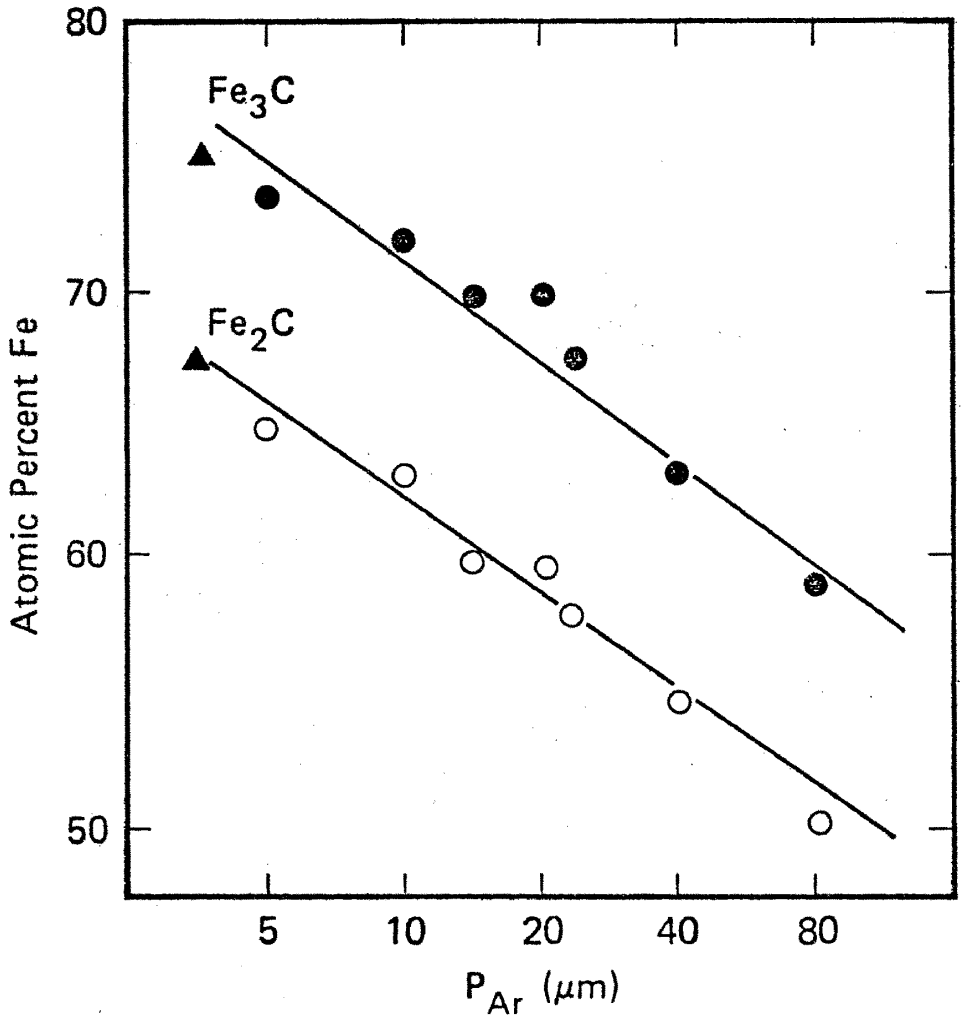

Fig. 4-1. The composition of amorphous FeC films as a function of deposition gas pressure. The solid circles are data obtained from a target of Fe_3C. The open circles are results when the target composition was Fe_2C. Note that the abscissa is on a log scale.

The room temperature $4\pi M$ of the Fe_xC_{1-x} films quite naturally decreases with decreasing Fe content. $4\pi M$=13100 gauss for x=0.75, dropping to $4\pi M$=6500 gauss for x=0.5. It is important to compare these results to those for Fe_xSi_{1-x} and Fe_xGe_{1-x}. One key feature is that, while $4\pi M$=6500 gauss for $Fe_{0.5}C_{0.5}$, both $Fe_{0.5}Si_{0.5}$ and $Fe_{0.15}Ge_{0.5}$ are paramagnetic at room temperature. The reason for the larger room temperature magnetization in the C based films appears to be due to both a larger moment per Fe atom and a higher T_c (i.e., stronger exchange coupling). The comparison is better understood with the aid of Fig. 4-2 where we plot the moment per Fe atom at 300K vs. x (the Fe concentration) for Fe_xC_{1-x} films. For comparison we have included the results for Fe_xSi_{1-x} and Fe_xGe_{1-x} films taken from reference 15 through 20.

For Fe_xC_{1-x} films the Fe moment decreases slowly to about $1.3\mu_B$/Fe atom at x=0.5. Note that in the region where the compositions of the films from the two targets overlap. We attempted to determine the Curie temperature (T_c) for these

films but found that in all cases (even for x=0.5) $T_c > 525K$. Since T_c is so high, one expects only a small difference between the room temperature moments and moment at zero Kelvin.

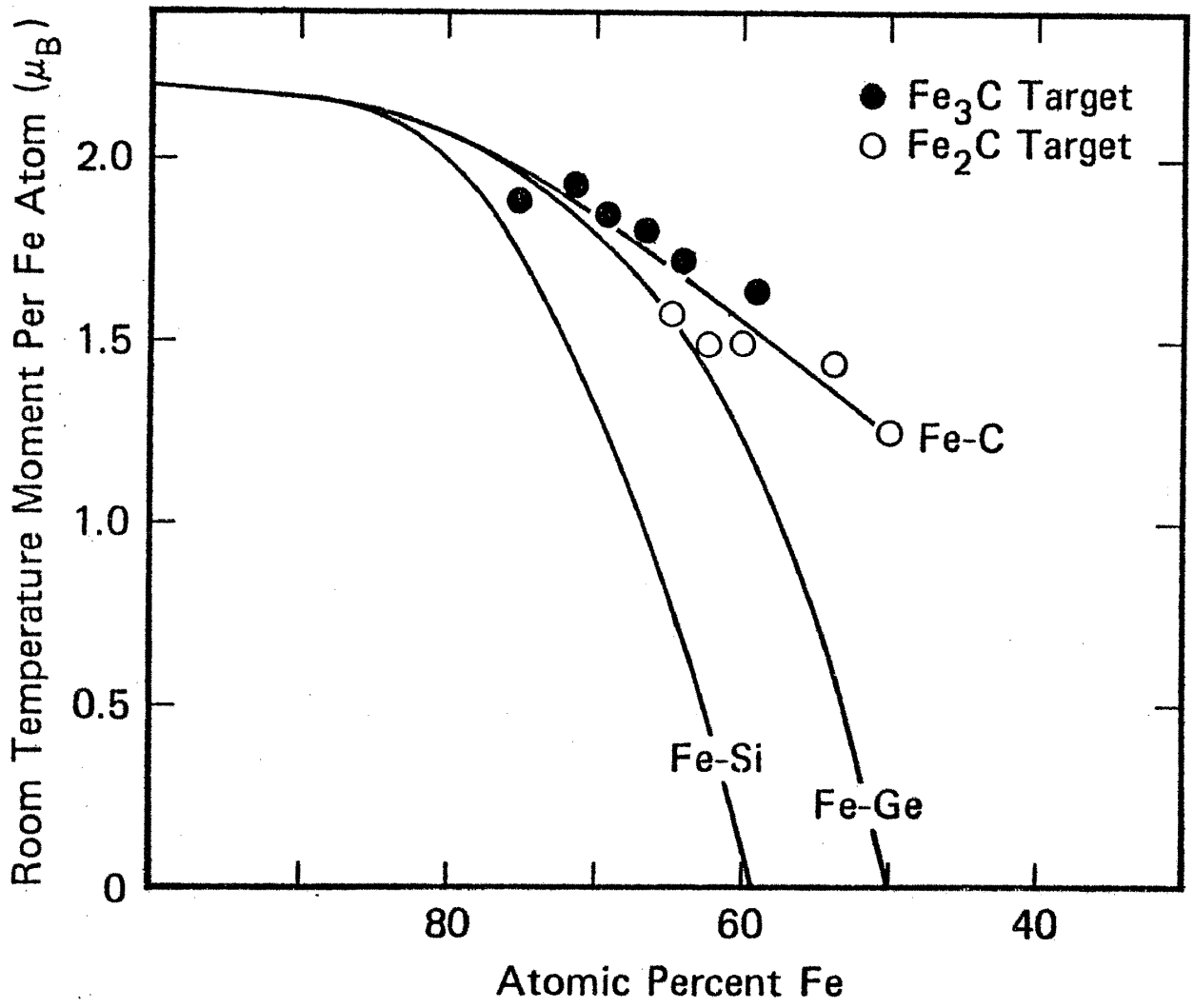

Fig. 4-2. The dependence of the room temperature Fe moment upon Fe concentration (x) for Fe_xC_{1-x}. Also included is data for Fe_xSi_{1-x} and Fe_xGe_{1-x} from Refs. 15 through 20.

In the case of the Fe_xSi_{1-x} films, the room temperature Fe moment disappears at $x \approx 0.59$. The data of Marchal et al.(16,17) shows that the low temperature Fe moment disappears at roughly the same value of x. Thus the Fe moment persists to much smaller x in the Fe_xC_{1-x} films. For Fe_xGe_{1-x}, the room temperature moment disappears near x=0.50, but the low temperature moment persists to $x \simeq 0.58$. In fact the low temperature moment for $Fe_{0.50}Ge_{0.50}$ of $1.5\mu_B$/Fe is on the order of that $Fe_{0.50}C_{0.50}$. So while the low temperature moments are similar in these alloys, T_c for $Fe_{0.50}Ge_{0.50}$ is near 260K whereas T_c for $Fe_{0.50}C_{0.50}$ is greater than 525K. Thus the exchange coulpling is considerally stronger in Fe_xC_{1-x} films.

B. COERCIVITY, ANISOTROPY AND MAGNETOSTRICTION

All films were found to have perpendicular anisotropy. Fig. 4-3 shows the coercivity (H_c) and the perpendicular anisotropy field H_k as a function of P_{Ar}. The variation in H_c and H_k are the result of the P_{Ar} deposition parameters and not a result of the accompanying composition variation. This was concluded from the fact that this same behavior for H_c and H_k was observed for other systems[21] (Fig. 4-4,5, Fe-Si-B, Fe-Cr-P-C) where composition changes do not occur. From the obvious correlation between H_c and H_k, it is probable that both H_c and H_k are stress induced in these films. We confirmed this possibility by annealing with large H_c (>5.0 Oe) and H_k (>400 Oe) and found that a 250°C anneal reduced H_c to below 1.0 and H_k to below 100 Oe.

Magnetostriction measurements were also carried out with an apparatus similar to that described Klockholm.[22] In general H_k was larger than the applied field. Thus we could obtain magnetostriction constants (Λ) only for films deposited with $P_{Ar} \approx 15\mu m$ (i.e., $x \cong 0.70$ and $x \cong 0.60$). Λ values were 1.3×10^{-5} and 1.0×10^{-5} respectively. By addition chromium and phosphorous it is possible in some cases to improve the corrosion resistance as well as rapid quenched samples.

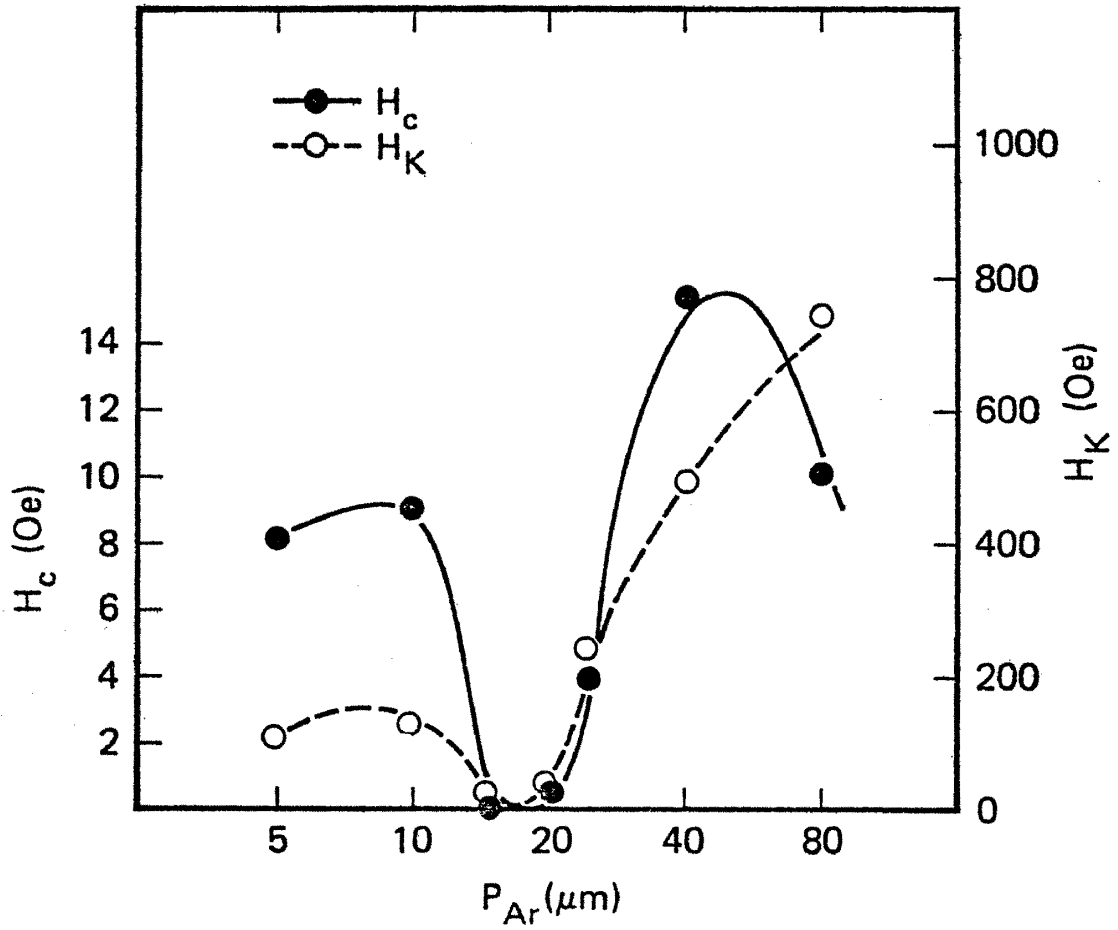

Fig. 4-3. This figure shows the dependence of the H_c and H_k on deposition gas pressure. The fact that both H_c and H_k go through a minimum at the same point indicates that these parameters are stress dependent. This observation has been confirmed by annealing studies. The minimum value for H_c was less than 100 mOe, which compares favorably with values obtained for bulk amorphous transition metal-metalloid alloys.

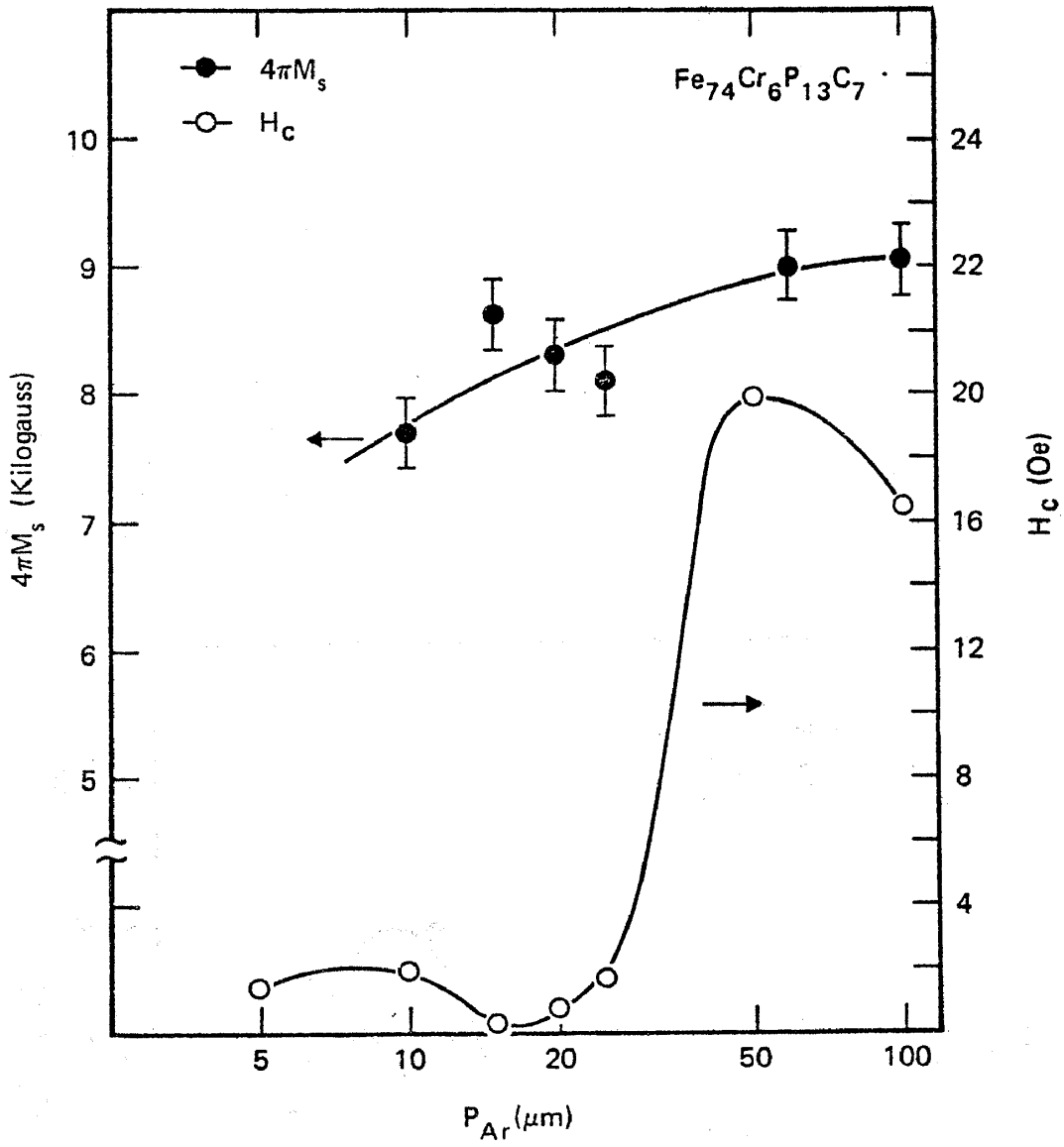

Fig. 4-4. This figure shows the dependence of $4\pi M_s$ and H_c on P_{Ar} for films deposited from a target of $Fe_{74}Cr_6P_{13}C_7$. The fact that $4\pi M_s$ does not change significantly with P_{Ar} confirms the microprobe results that, unlike the FeC system, the composition of FeCrPC films do not vary with P_{Ar}. Note. however, that H_c goes through a minimum at the same value of P_{Ar} as was the case for the FeC film.

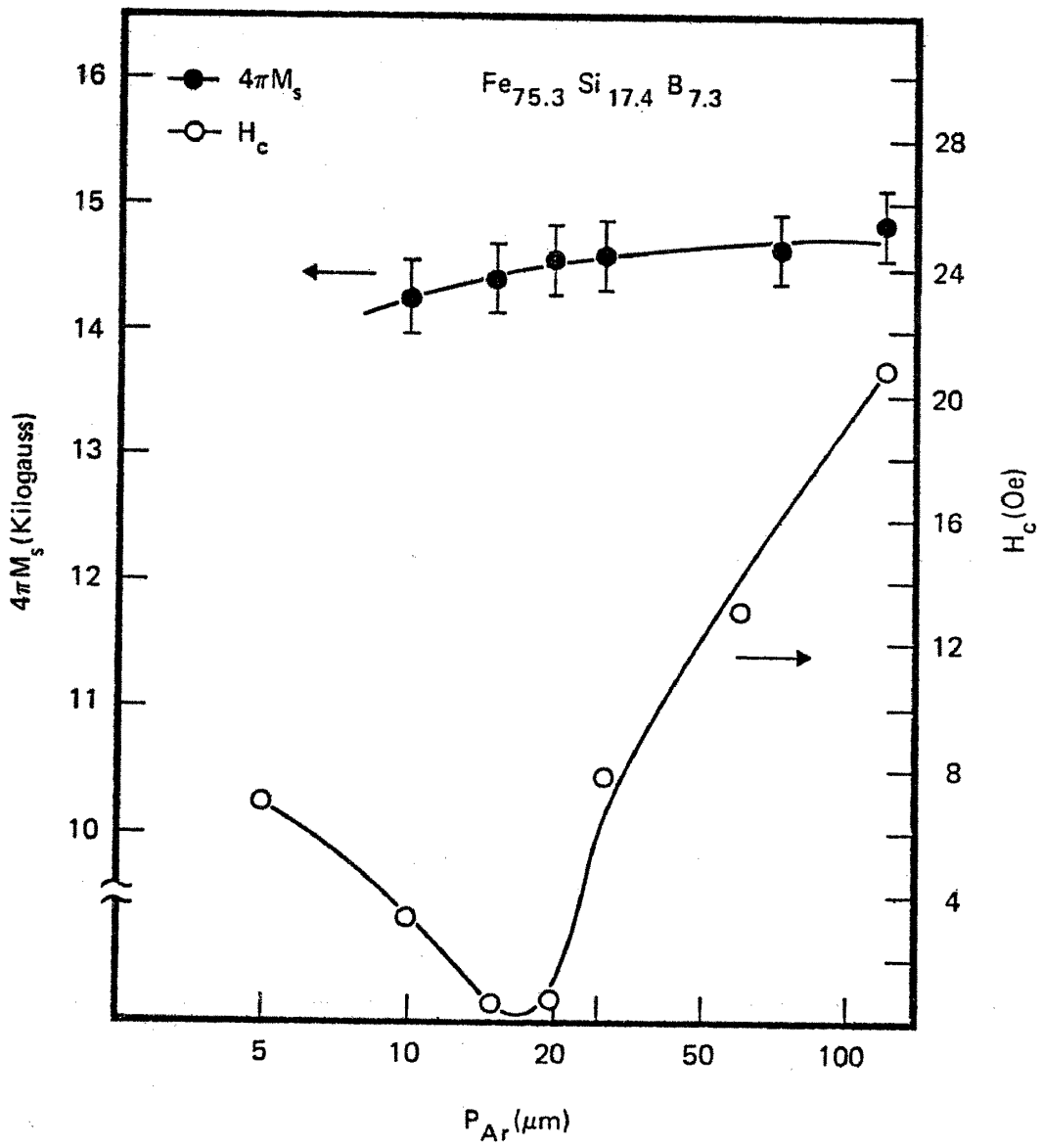

Fig. 4-5. This figure shows $4\pi M_s$ and H_c for FeSiB films. Note that the results are similar to those in Figs. 4-3 and 4. H_c goes through a minimum near $P_{Ar} \approx 15$ μm, while $4\pi M_s$ does not depend on P_{Ar}.

§5. EFFECTS OF SUBSTRATE BIAS AND ANNEALING ON THE PROPERTIES OF AMORPHOUS GdCo, GdFe and GdCoX FILMS

We have examined the dependence of various properties of amorphous films upon substrate bias (Vb) and annealing. For GdCo alloy system, uniaxial anisotropy (Ku) is maximum at Vb=-200V. Increases in Vb causes Ku to decrease so that Ku≈ 0 for Vb=-400V as shown in Fig. 5-1.

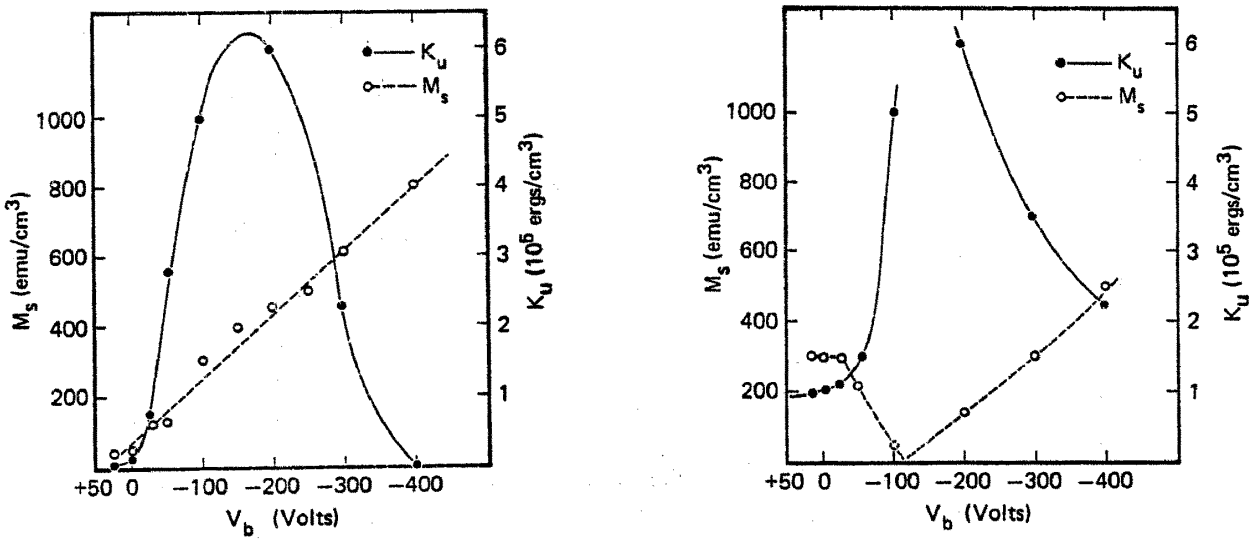

Fig. 5-1. The figures show the results for the uniaxial anisotropy energy, Ku and the saturation magnetization, Ms, as a function of substrate bias for films sputter deposited from a target of composition (a) $Gd_{22}Co_{78}$, (b) $Gd_{28}Co_{72}$.

Furthermore the Ar content of the films reaches a maximum for Vb≈200V. Since Ku is not a monotonic function of Vb, it does not correlate directly with Vb nor Co or Gd contents of the films; however these does appear to be a very strong correlation between Ku and Ar content of a film but only for the amorphous GdCo alloy system, not for the amorphous GdFe alloy system.

X-ray diffraction patterns (see Fig. 5-2) appear to correlate with Ku. In particular a shoulder whose intensity is roughly proportional to Ku does develop on the low angle side of the profile for all films in the amorphous GdCo binary system.

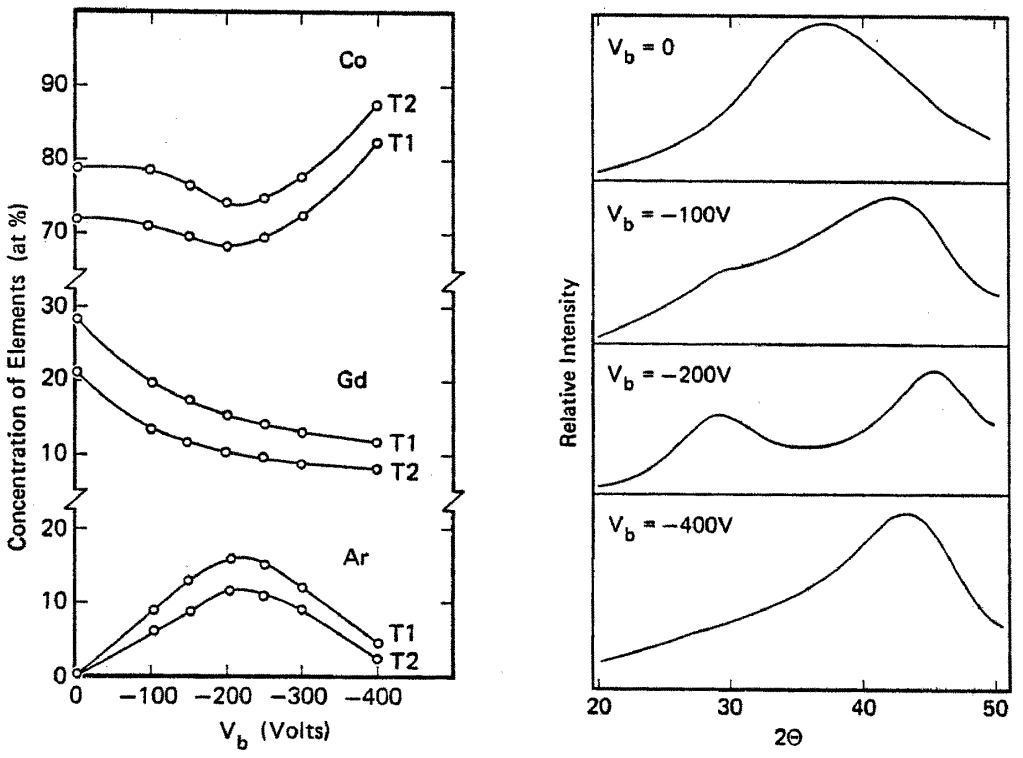

(a) (b)

Fig. 5-2. The figure (a) illustrates the effects of substrate bias on film composition. The curves labeled T1 and T2 are the data for target 1 ($Gd_{28}Co_{72}$) and target 2 ($Gd_{22}Co_{78}$) respectively. The figure (b) shows the CuK_α x-ray diffraction profiles for target 1. Note that the intensity at $2\theta \approx 27.5$ scales approximately with Ku and Ar concentration.

The result for the GdFe system were different, i.e., Ku was large for Vb>0 but decreased rapidly with negative bias. GdCoX films were similar to GdCo films except that the x-ray diffraction patterns showed little dependence on Vb.

The final point is with regard to the effects of annealing. GdCoMo films undergo no change in both Ku and Ms on standard annealing (200°C for 4 hours in a vacuum better than 10^{-7} torr). The binary films (GdCo, GdFe system) experience a decrease only in Ku by about factor of two. For GdCoCu and GdCoAu films both Ku and Ms are reduced dramatically. The addition of a few atomic percent Mo stabilizes the films against the annealing effects. This could be explained by the difference in the nature of the chemical bonding of Mo and Cu(Au) with GdCo alloys. For example, in crystalline alloys the noble metals Cu and Au are insoluble in Cu while Mo forms many compounds with both Co and Gd. This difference in chemical affinity would carry over into the amorphous phase as well, even though the constraints on solubility are relaxed.

REFERENCES

1). N. Heiman and K. Lee, A.I.P. Conf. Proc. 34 319 (1976).

2). K. Lee and N. Heiman, A.I.P. Conf. Proc. 24, 108 (1975).

3). H.A. Alperin, J.R. Cullen and A.E. Clark, A.I.P. Conf. Proc. 29, 186; 1975 M^3 Conf., Phila.

4). J.R. Cullen paper for Int'l Conf. on Magnetic Alloys and Oxides (ICMAO). Technion-Haifa. Israel 15-18 August 1977.

5). N. Heiman, K. Lee, R.I. Potter, and S. Kirkpatrick, J. Appl. Phys. (to be published).

6). N. Heiman, K. Lee, and R.I. Potter, 21rt Annual Conference on Magnetic Materials-1975.

7). Data for crystalline alloys were obtained from K. Taylor, Advan. Phys. 20, 551 (1971) and references cited therein.

8). See for example N. Mott in Metal-Insulator Transitions, Barnes and Noble (London 1974), p.94.

9). T.R. McGuire, R.C. Taylor, and R.J. Gambino, A.I.P. Conference Proceedings 34, 346 (1976).

10). N.S. Kazama, M. Kameda and T. Masumoto, A.I.P. Conference 34, 307 (1976).

11). T. Mizoguchi, T.R. McGuire, R.J. Gambino and S. Kirkpatrick, Physica 86-88B, 783 (1977).

12). K. Lee and N. Heiman, A.I.P. Conf. Proc. 24, 108 (1975).

13). R. Boucher, 1977 Intermag Conference (to be published).

14). J. Durand and S.J. Poon, 1977 Intermag Conference (to be published).

15). Y. Shimada and H. Kojima, J. Appl. Phys. 47, 4156 (1976).

16). G. Marchal, Ph. Mangin and Chi. Janot, Solid State Comm. 18, 739 (1976).

17). G. Marchal, Ph. Mangin, M. Piecuch and Chi. Janot, J. Physique. C6, 763 (1976).

18). G. Suran, H. Daver, J.C. Bruyere, A.I.P. Conf. Proc. 29, 162 (1976).

19). G. Suran, H. Daver, J. Sytern, Physica 86-88B, 810 (1977).

20). G. Suran, H. Daver, J. Sytern, A.I.P. Conf. Proc. 34, 310 (1976).

21). N. Heiman, N.S. Kazama, and R. Hempstead, submitted IBM Journal of R & D.

22). E. Klockholm, IEEE Transactions on Magnetism 12, 819 (1976).

23). J.M.D. Coey, S. von Molnar and R.J. Gambino, Solid State Comm. 24, 167 (1977).

More detailed data and extended reports will be appear in the following journals.

§1. N. Heiman and N.S. Kazama,"The magnetic properties of amorphous alloys of Fe with La, Lu, Y and Zr", submitted to Phys. Rev.

§2. N. Heiman and N.S. Kazama,"The concentration dependence of the Co moment in amorphous alloys of Co with Y, La and Zr", to be published in Phys. Rev.

§3. N. Heiman and N.S. Kazama,"Magnetization of amorphous RE_x-Cu_{1-x} alloys (RE=Gd, Tb, Dy, Ho)", to be published in AIP Conf. Proc. (1977) Minneapolis.

§4. N.S. Kazama and N. Heiman,"Magnetic properties of amorphous FeC thin films", to be published in AIP Conf. Proc. (1977) Minneapolis.

§5. N. Heiman, N.S. Kazama, D.F. Kyser and V.J. Minkiewicz, "Effects of substrate bias and annealing on the properties of amorphous GdCo, GdFe and GdCoX films", to be published in J. Appl. Phys.